WWW.IJRPR.COM

International Journal of Research Publication and Reviews

Journal homepage: www.ijrpr.com ISSN 2582-7421

CFD Simulation of a Curved Solar Air Heater with Various Shaped Down Turbulators

Ankit Kumar[1], Prof. Shahrukh Khan[2]

[1]Trinity Institute of Technology and Research, Research Scholar, RGPV Bhopal, MP, INDIA
[2]Trinity Institute of Technology and Research, Professor, RGPV Bhopal, MP, INDIA

ABSTRACT

Curved designs of solar air heater ducts outperform flat plate SAH designs in terms of thermal properties, however the former shows a little drop in hydraulic efficiency. The centrifugal action causes the formation of secondary vortices, which results in the mixing flow. Furthermore, the formation of dean vortices accelerates heat transmission in curved SAH. These findings are not found in flat plate SAH.To explore the heat transmission and flow behaviour, a three-dimensional CFD simulation was performed in a curved duct of a solar air heater with an upper roughened wall and down-configuration ribs of half triangular, whole triangular, and semi-circular shapes. The heat transmission physiognomies of a curved duct of a solar air heater were studied using the simulation programme ANSYS 17.0.In comparison to half-triangular and semi-circular ribs, the curved solar air heater with triangular rib roughness on the absorber plate has been proven to produce better results and may be utilised to promote heat transmission. Triangular-shaped ribs are shown to have the greatest increase in Nusselt number, which is 1.112 times that of half-triangular and corresponds to a Reynolds number of 15,000 for the tested range of parameters.

Keywords: Artificial roughness, shape of rib, curved solar air heater, heat transfer, friction factor, and CFD.

I.INTRODUCTION

Any device's ability to transfer heat depends on how the fluid interacts with the heated surfaces within the passageway and how the flow channel is set up. The arrangement of the absorber plate and the flow-through duct has a significant impact on the performance of the solar air heating system [1, 2]. This is the reason that many researchers have based their research on various SAH structure components, particularly the absorber plate and the duct that incorporate various rib or turbulator shapes, such as circular and square cross-section ribs, tapered rectangular cross-sections, different combinations of V-shaped ribs, wavy delta winglets, anchor-shaped inserts, perforated winglet vortex generators, etc.

It is now vital to create efficient designs for equipment that uses renewable energy sources, such as solar energy, due to the high costs associated with producing energy through the use of non-renewable fuel resources, such as coal, crude oil, etc. [3]. Since flat plate SAH is frequently used in a wide range of home and industrial applications, including space heating, agricultural crop drying, desalination, and other heating applications, enhancing designs for improved thermal efficiency can significantly help meet our growing energy demands.

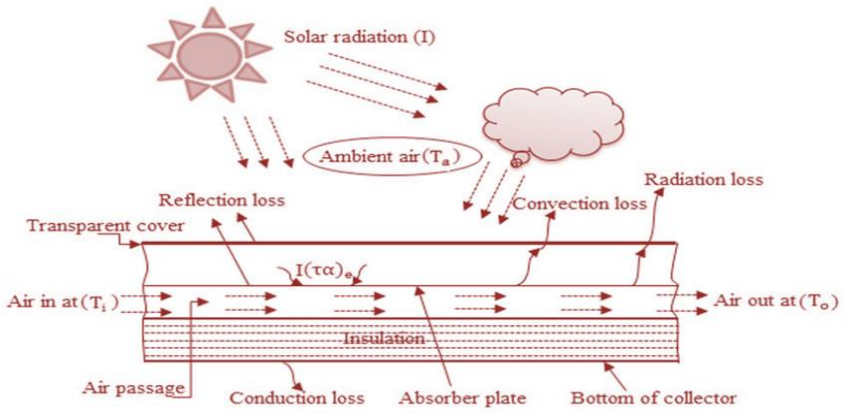

Figure 1. Schematic diagram of conventional solar air heaters

Additionally, the SAH must be thermally efficient in order to utilise the entire amount of useable solar energy, given that there are only around 4-6

hours of sun insolation each day. The absorber plate and the flow duct, where cold air enters, produces energy from the heated plate, and exits the channel, are two crucial components of the SAH design [4]. Due to the isolation of the flow and the reattachment between the successive corrugations, which decrease thermal resistance and increase heat transfer rate, the use of ribs or grooves on the inner surface of the heat exchangers was one of the common passive approaches to break down the laminar sub-layer and create a turbulent local wall. The main goal of the current study is to determine how flow and roughness factors affect the typical heat transfer and flow friction properties of a curved solar air heater that has been intentionally roughened and integrated with various shaped ribs.

Curved solar air heater duct designs have significantly better thermal properties than flat plate SAH designs, although the former exhibits a minor drop in hydraulic efficiency. Curved SAH shows how the centrifugal action causes secondary vortices to form, resulting in the mixing flow. Furthermore, the development of dean vortices accelerates heat transmission in curved SAH. These findings are not present in flat plate SAH.

2. LITERATURE REVIEW

2.1. Previous work

The availability of energy is a major problem in daily life under the current system. Due to the depletion of traditional energy sources and the environmental dangers they pose, a quantitative technique is required to anticipate the supply of energy. Solar energy is a practical and affordable renewable energy source that can meet the world's rising energy needs. The flat plate solar air heaters (SAHs) are simple devices with little thermal maintenance requirements. SAHs are often used for a variety of residential and industrial applications, including room heating, the drying out of agricultural products, the heating of industrial items, the seasoning of wood and other materials, etc.

The SAH's poor performance as a result of the lesser air transport capacity is one of its main issues. Instead of being transferred to the flowing air, a significant percentage of the thermal energy from the absorber plate is lost to the surrounding environment. Different approaches to solving issue have been described by researchers. The desire to apply different active or passive strategies to improve the thermo-hydraulic efficiency (THEP) of SAH has grown significantly during the past few years. The whole turbulent flow created and the local turbulence generated in these systems are the main targets of the active approach. The surface shape of the improved and modified absorber serves as the foundation for the passive approach.

We might include the research of Alam and Kim (2017), Kalogirou et al. (2016), Sharma, and Kalamkarar among these research pieces, as well as significant review papers addressing theoretical, computational, and experimental investigations for new suggested and improved solar air heater prototypes (2015).

Alam and Kim (2017), for instance, provided a study of SAH collectors using various criteria and ribs. They proposed that while forced artificial roughness increased Nusselt volume, it also increased pressure drop [1].

Kalogirou et al. (2016) identified a variety of collector types in their analytical report, with the first classification being a parabolic dish and parabolic trough collector and the second classification including SAH, evacuated tube collectors, and flat-plate collectors. They discovered that the exergy analysis provides a useful method for examining and evaluating the various SAH configurations [2].

Sharma and Kalamkar (2015) later reported that there are several geometric structures that can be used to facilitate the heat transfer in SAH, including artificial roughness, baffles, ribs, fins, and various shapes and configurations of groves. They also provided a detailed thermal hydraulic efficiency study of artificially roughened collectors. Additionally, they claimed that the use of a constrained turbulator height enhanced the quantity of Nusselt turbulators and decreased pressure loss [3].

Arunkumar, Karanth, and Kumar carried out a review study of SAH with different artificial roughness geometry (2020). The results showed that increasing the roughness of the ribs in turbulators increases both the friction factor and the temperature of the exit air. However, when the quantity of Re grows, the THEP of the SAH drops [4].

A SAH with a double airflow pass and multiple C shape roughness on the heated wall was the subject of an experimental investigation by Gabhane and Kanase-Patil (2017). For a fixed height ratio (e/D = 0.02), the parameters of a duct aspect ratio (W/H) of 10 and a rib pitch ratio (P/e) ranging from 8 to 40 are taken into account. The largest increase in heat transmission (approximately 2.8 times compared to the smooth plate solar heater) and lowest friction factor are found with a pitch ratio of 24 [5].

Anil Singh Yadav and **J.L. Bhagoria (2017)**performed an analysis on a SAH with square-sectioned transverse ribs considered at the underside of the top wall, where continuous heat flux conditions are applied, a numerical investigation is performed to examine the heat transport and flow friction characteristics. The influence of the relative roughness pitch was investigated on the average number of Nusselt, the average friction factor and the thermohydraulic efficiency parameter (THPP). Relative roughness pitch in the range of $7.14 \leq P/e \leq 17.86$ and relevant Reynolds numbers in the range of $3800 \leq Re \leq 18{,}000$ are protected by this inquiry. With the finite volume process, the two-dimensional steady, turbulent flow, and heat transfer governing equations are solved. In order to analyse the overall influence of the relative pitch of roughness, the THPP under the same pumping power constraint is determined. The overall THPP of 1.82 for the existing set examined is obtained by using the ribs with a P/e of 10.71 [6].

Alam et al. (2014) conducted an experimental investigation to compare the Nusselt number and friction losses for a SAH with non-circular holes, such

as rectangular and square kinds, that are positioned on the V-shaped obstructions. Results have demonstrated that maximum flow resistance and Nu number are attained for relative pitch P/e = 8 and 4, respectively. Thermal increase is possible in the case of a rectangular hole with a circularity of 0.69 and an attack angle close to 60 ° [7].

A SAH experimental research was performed by **Aldabbagh** and **Egelioglu (2015)** to test the fluid flow and thermal behavior for single and double-pass airflow with transverse fin for various mass flow values ranging from 11×10^{-3} to 32×10^{-3} kg/s with an angle of inclination of 37 °. In contrast with the single-pass SAH, the authors concluded that double-pass channel thermal efficiency and flow resistance were also higher [8].

Poongavanam et al. (2018) used a SAH with a modified surface with a form of V-corrugation to perform an experimental analysis of the impact on the Nu number and the pressure drop levels of a rectangular duct of the induced disturbances and enhanced turbulence. They found that the thermal efficiency of the SAH is highly dependent on the absorption of V-corrugation and solar radiation by the SAH. Compared to the smooth absorber layer, the results showed an improved SAH performance with an ideal THEP in the range of 1.35 to 1.56 times [9].

We may cite the work of **Yang** and **Chen (2014)** for numerical studies, who carried out an optimization technique to numerically evaluate a SAH with a vertical partition wall along the absorber plate at the top end. The authors concluded that, relative to the smooth collector, the presence of the partition provides high output and those dimensionless partition parameters such as length (L), thickness (W) and pitch (A) play an important role in the control of the THEP [10].

Gilani et al. (2017) proposed new conical pin protrusions form turbulators to increase the thermal performance of a SAH. The results showed that the ideal inclination value was 45 degrees. Compared with the smooth duct, a rise of up to 26.5% was achieved for the THEP for the roughened wall [11].

Priyam offered a theoretical analysis of SAH with transverse wavy fins attached to the heated top surface (2017). Results showed that the THEP reduces as the collector length increases with a high pressure drop [12].

Yadav et al. (2020) have completed a theoretical research of artificially roughened SAH using arc-shaped wires organised under the solar collector's operational parameters. The results demonstrated that the gain in thermal efficiency for a parallel flow in rough SAH is considerable and can reach a value of roughly 8 percent to 10 percent [13] comparing to the smooth absorber scenario.

According to research by Ajeet et al. (2020), thermo-hydrodynamically curved solar air heaters (SAH) perform better than flat SAH designs. Additionally, it has been shown that down-configurations of turbulators or extended surfaces on a flat plate solar collector considerably increase thermal efficiency. Half-trapezoidal and quarter-circular shape ribs were shown to increase thermal performance to the greatest extent, by 17 and 16 percent, respectively, however when compared to trapezoidal shape ribs, quarter-circular rib frictional loss was found to be around 10 percent less [14].

2.2. Problem finding of literature review

After undertaking a systematic literature review, it is noted that many experimental and computational studies were carried out using artificial roughness in the field of improved thermal efficiency of solar air heaters. However, several C-shape, single and double-pass flow with transverse fin, V-corrugation, delta, stepped cylindrical, oval, square and rectangular ribs were studied in most of the studies studied. Owing to the variation in the shape of the rib and the flow structure, that shows the susceptibility of each design to these parameters, multiple studies note varying degrees of improvements in heat transfer and friction factor. Therefore, the purpose of heat transfer improvement with minimal pressure loss penalty must be based on the choice of any preferred roughness shape and therefore a thermo-hydraulic performance analysis is required.

It is evident from the above discussion that studies are scarce on curved SAH fitted with ribs, which inspired the authors to conduct the present study to investigate the best rib designs for higher thermo-hydraulic efficiency.

In this study, a three-dimensional CFD analysis was performed in a curved solar air heater duct with a roughened top wall and down-configured ribs with half-triangular, full-triangular, and semi-circular shapes to examine the flow and heat transfer behaviour. For the investigation of the heat transmission physiognomies of a curved duct of a solar air heater, the simulation tool ANSYS 17.0 was utilised.

The main objective of the present studies is:

- The effect of roughness and flow parameters in a Curved duct of a solar air heater with a upper roughened wall with down-configuration ribs having shape of half triangular, full triangular, and semi-circular on average heat transfer and flow friction properties of artificial rugged solar air heaters.
- To figure out the optimum rib configuration for heat transfer enhancement.
- Investigate the effect of roughness parameters on different SAH thermal properties, such as the number of Reynolds, the number of Nusselt, and the flow friction factor.

3.COMPUTATIONAL MODEL

3.1. Geometrical details of computational model

In order to perform the simulation study, Ajeet et al. (2020) [14], a research researcher with precise sizes, provided the geometry. Table 1 and Figure 2 respectively display the geometry and computational model features of conventional design.

Table 1 Geometric parameters of Curved solar air Heater

Geometrical parameters	Value / Range
length of duct, (mm)	1600
Duct height, H (mm)	40
Curvature angle (◦)	25
Duct hydraulic diameter, D_h (mm)	33.33
Rib height e (mm)	1.4
Pitch P (mm)	50
Relative groove height ratio, 'e/H'	0.125

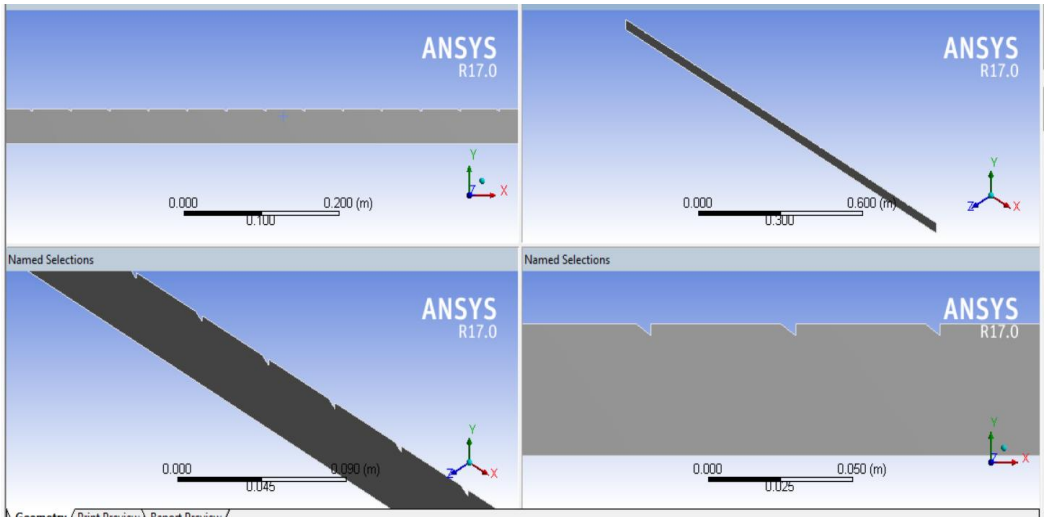

Figure 2. Geometry of a curved SAH having25° curvature angle with the half-triangular grooved absorber plate (Conventional design).

After than in the proposed designs, 'full triangular and semi-circular' section rib is employed on the absorber plate. The part of the model designed in ANSYS (fluent) workbench 17.0 software.

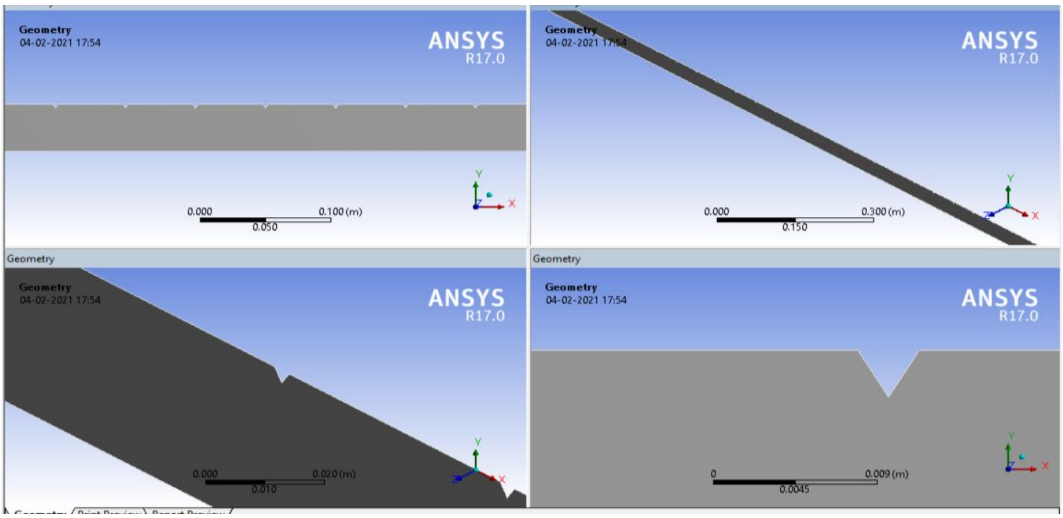

Figure 3. Geometry of a curved SAH having25° curvature angle with the triangular grooved absorber plate (Proposed design).

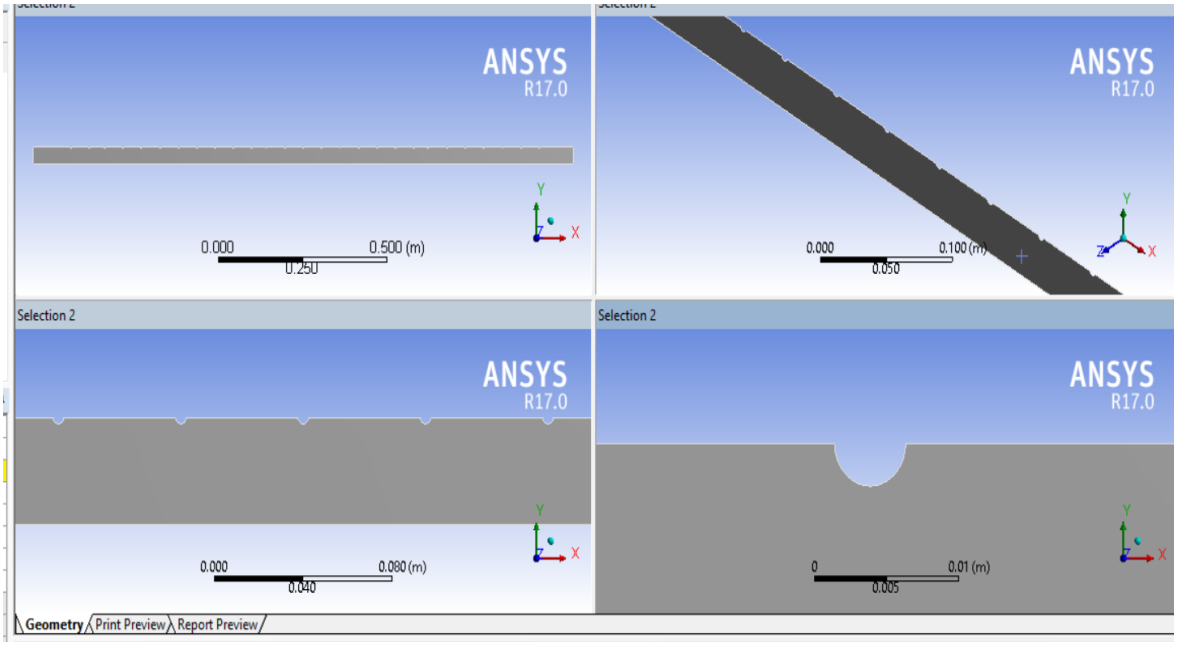

Figure 4. Geometry of a curved SAH having25° curvature angle with the semi-circular grooved absorber plate (Proposed design).

3.2. Meshing

In the pre-processor step of ANSYS FLUENT R 14.5, a three-dimensional discretized model was developed. Although the styles of grids are connected to simulation performance, the entire structure is discretized in the finite volume by, default; a coarse mesh is generated by ANSYS software. Mesh contains mixed cells per unit area (ICEM Tetrahedral cells) having triangular faces at the boundaries. The meshing that has used in this analysis is mesh metric with medium smooth curvature.

Table 2. Meshing detail of various models

S. No.	Parameters	Semi-triangular rib (Conventional design)	triangular rib (Proposed design	Semi-circular rib (Proposed design)
1	Curvature	On	On	On
2	Smooth	Medium	Medium	Medium
3	Number of nodes	64767	64808	64943
4	Number of elements	63134	63174	63207
5	Mesh metric	None	None	None
6	Meshing type	Tetrahedral	Tetrahedral	Tetrahedral

4. NUMERICAL PROCEDURE

The RNG k-ε model was chosen as the turbulence model for the further study of the problem because the flow is turbulent. As a heat transfer model, the energy equation is also kept ON.The numerical model for fluid flow and heat transferthroughanartificiallyroughenedsolarairheater is developed under the followingassumptions:

- The fluids sustain a single-phase, turbulent flow through the duct.
- 3D steady heat transfer fluid flow.
- Flow thoroughly formed both thermally and hydraulically (steady-state conditions).
- Both the fluid (air) and rigid absorber (aluminium) have continuous thermo-physical characteristics (temperature independent).
- Refused heat transfer by radiation.

The heat transfer equations and fluid flow structure contains the mass, momentum and energy conservation equation. The equations are as follows:

The mass conservation:

$$\frac{\partial(\rho u_i)}{\partial x_i} = 0$$

The momentum conservation:

$$\frac{\partial\left(\rho\overline{u_i}\,\overline{u_j}\right)}{\partial x_j} = -\frac{\partial \bar{P}}{\partial x_i} + \frac{\partial\left(\mu + \mu_t\left(\frac{\partial \overline{u_i}}{\partial x_j} + \frac{\partial \overline{u_j}}{\partial x_i}\right)\right)}{\partial x_j}$$

The energy conservation:

$$C_p\overline{u_i}\frac{\partial(\rho\bar{T})}{\partial x_i} = \frac{\partial\left(\lambda\frac{\partial \bar{T}}{\partial x_i}\right)}{\partial x_i} - C_p\frac{\partial\left(\frac{\mu_t}{Pr_t}\frac{\partial \bar{T}}{\partial x_i}\right)}{\partial x_i}$$

All governing equations are discretized by a second-order upwind-biased scheme using a finite volume approach and then solved in a segregated manner. The SIMPLE algorithm to couple pressure and velocity is selected for theincompressibleflowcomputation. Convergence criteria are defined as 0.001 for all dependent variables. Whenever issues of integration are found, the solution starts with the upwind discretization system of first order and ends with the upwind system of second order.

Aftersettingallnecessaryinputconditions, theproblemissettoiteratefor1000iterationswithinwhich it gives well converged according to the set convergence criteria so that we can get accurate results.

4.1 Material Property

For any kind of analysis property are the main things which must be defined before moving further analysis .There are thousands of materials available in the ANSYS environment and if required library is not available in ANSYS directory the new material directory can be created as per requirement.

Table 3. Thermo-physical Properties of Air and Aluminium

Properties	*Air*	*Absorber plate (Aluminium)*
Density, 'ρ' (Kg/ $m^{3)}$	1.184	*2719*
Specific heat, 'c_p' (J-Kg/K)	1003.62	*871*
Thermal conductivity, 'k'(W/ m-K)	0.026	*202.4*
Viscosity, 'μ' (N-s/m^2)	1.855×10^{-5}	---
Prandtl number	0.71	---

4.2. Boundary Conditions

All the cases considered were simulated under a set heat flux absorber value, q=1000 W/m^2. A flow velocity value corresponding to a basic Reynolds number, Re was assigned. At the outlet section, the atmospheric condition was maintained by assigning the gauge pressure value to zero (i.e. atmospheric condition) and rest walls were believed to be adiabatic (i.e. assuming no heat loss to ambient). The walls are subject to the boundary state of no-slip. For the Re 11,000-15000 scale, each case has been simulated. The flow was known as an incompressible flow, meaning that the density of the fluid was independent of changes in the pressure values.

For inlet flow to the duct and the outlet flow from the duct is regulated by a uniform velocity inlet boundary state. The air reaches the duct with a uniform velocity at room temperature (T_0 = 300 K) (U_0). A pressure outlet condition with fixed atmospheric pressure of 1.013×10^5 Pa is applied at the exit.Impermeable boundary and slip-free wall conditions over the walls of the duct are applied.

5. RESULTS AND DISCUSSIONS

The purpose of the present work of CFD is to research the impact that a rib shape has on average Nusselt numbers as well as average friction factor, and THPPs on the underside of the absorber plate in artificially roughened solar air heaters with transverse ribs.

The average Nusselt number for artificially roughened solar air heaters is defined as:

$$\boldsymbol{Nu = \frac{h\,D_h}{K_a}}$$

Reynolds number is defined as:

$$\boldsymbol{Re = \frac{\rho u D_h}{\mu}}$$

where $\boldsymbol{\rho}$ is the density of the air inlet, $\boldsymbol{u}$ is the average velocity of the air inlet, $\boldsymbol{D_h}$ is the hydraulic diameter of the wedge duct inlet, and $\boldsymbol{\mu}$ is the dynamic viscosity of air at the inlet.

For artificial solar air heaters the average friction factor is determined by:

$$\boldsymbol{f_r = \frac{\left(\frac{\Delta P}{l}\right) D}{2\rho \vartheta U^2}}$$

Where $\boldsymbol{\Delta P}$ is pressure drop across the duct of an artificially roughened solar air heater.

The temperature factor for artificially roughened solar air heaters is defined as:

$$Temperature\ factor = \frac{T_o - T_i}{I}$$

5.1. CFD validation

Computational models offer thorough and extremely reliable findings. However, it is necessary to verify numerical simulations of physical dimensions. To validate the numerical model, artificially roughened solar air heaters were simulated. The findings were compared to those by Ajeet et al. (2020) [14], who investigated the effects of semi-down turbulators on heat transmission and curved roughened frictional factors.

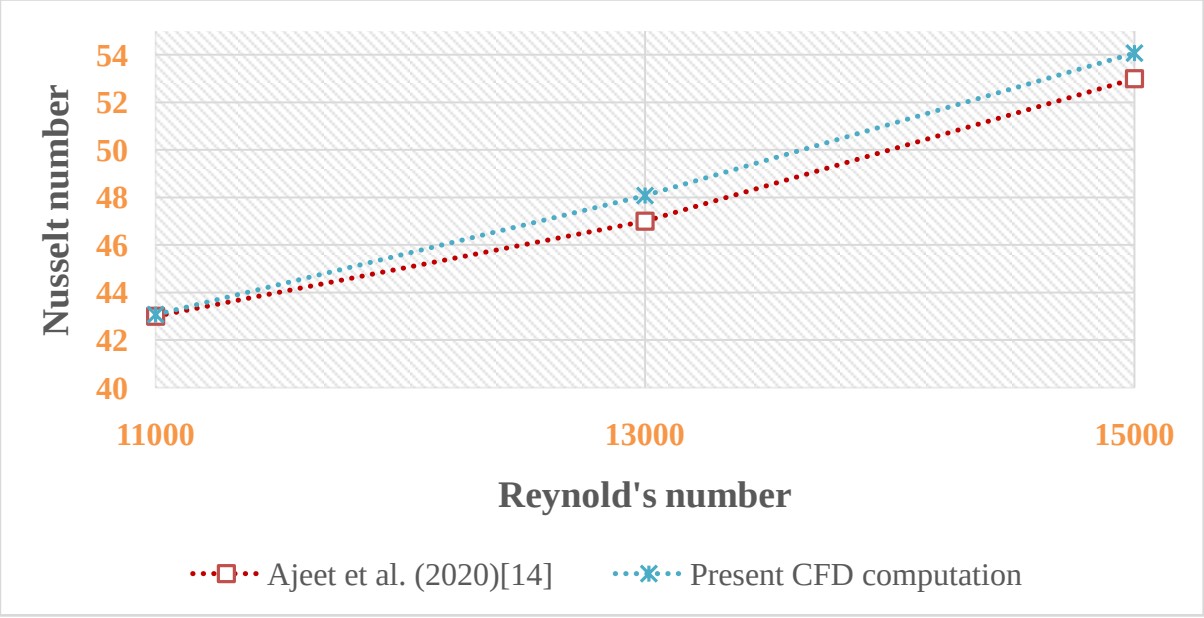

Figure 5. Comparison of the Nusselt number derived from CFD results and the Ajeet et al. (2020) [14] results.

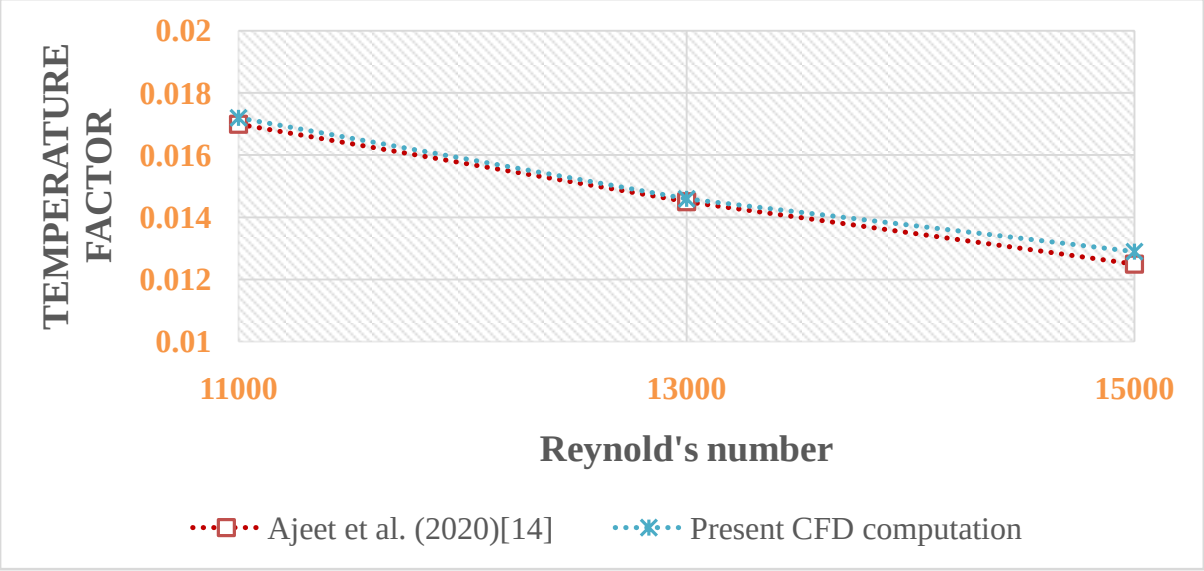

Figure 6. Comparison of the temperature factor values derived from CFD results and the Ajeet et al. (2020) [14] results.

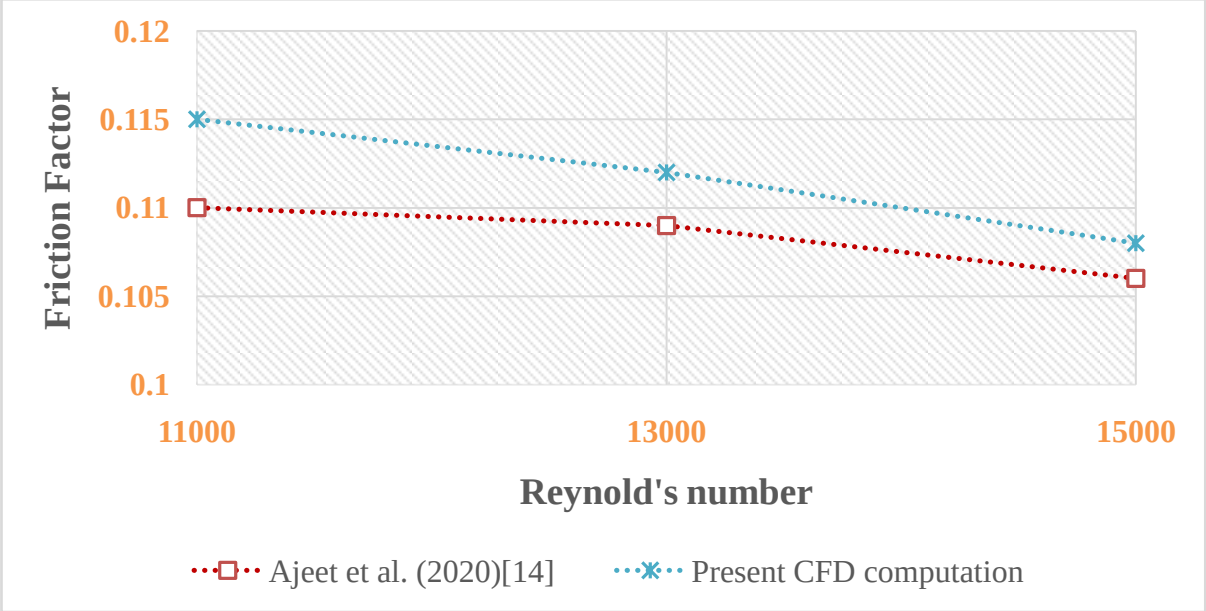

Figure 7. Comparison of the friction factor values derived from CFD results and the Ajeet et al. (2020) [14] results.

From the above graph, it is found that the value of **Nusselt number, Friction factor**, and **Temperature factor** calculated from numerical analysis is closer to value **Nusselt number, Friction factor**, and **Temperature factor** obtained from the base paper, which means that numerical model is correct.

5.2. Comparison between the value of the Nusselt number, Friction factor ratio, and Temperature factor for half-triangular, triangular, and semi-circular rib on the absorber plate

This section compares absorber plates with half-triangular, triangular, and semi-circular ribs on the absorber plate in order to clarify prior understandings and to distinguish the contribution that each of these shapes makes to the overall thermal increase of the proposed design.

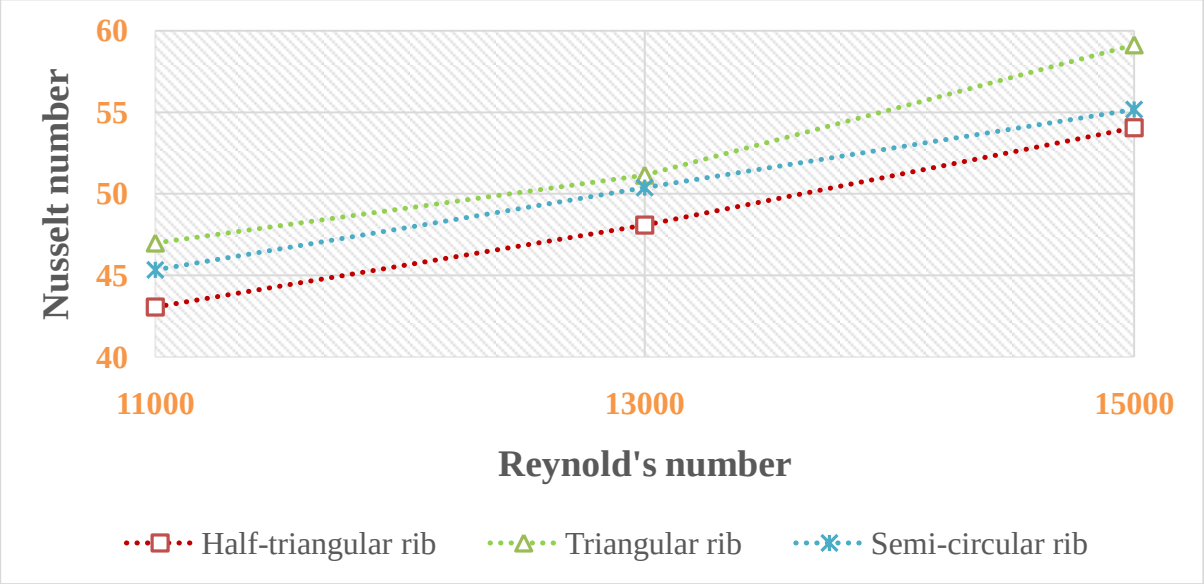

Figure 8. Comparison of the Nusselt number values with half-triangular, triangular, and semi-circular rib on the absorber plate

Figure 8. shows the variation of Nusselt number as a function of Reynolds number. In this case, the Nusselt number ratio increases with increase in Reynold's numberforallthecases.

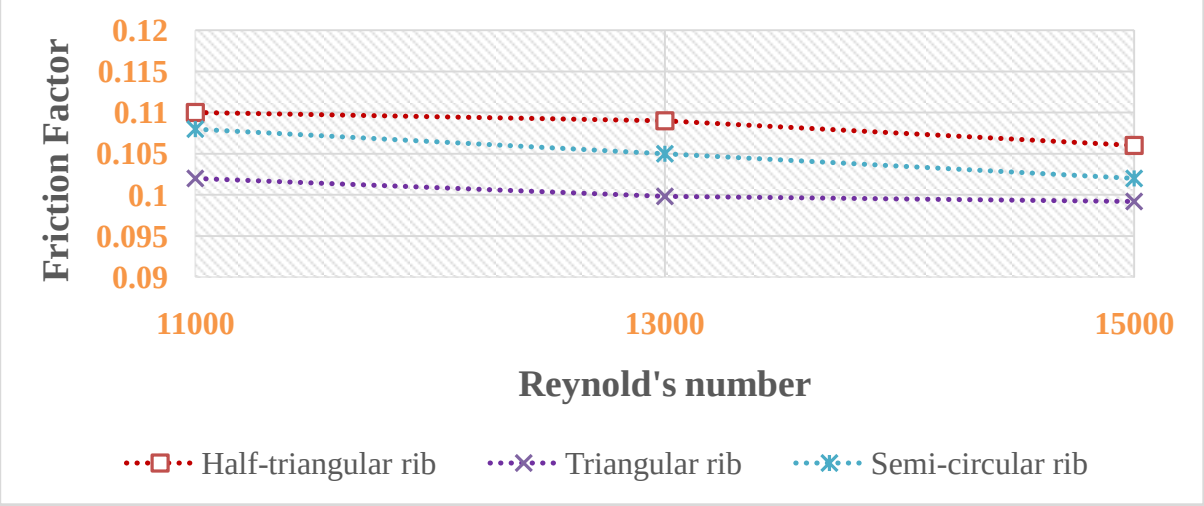

Figure 9. Comparison of the friction factor values with half-triangular, triangular, and semi-circular rib on the absorber plate

Figure 9 shows the variation of friction factor as a function of Reynolds number. In this case, the friction factor ratio decreases with increase in Reynold's numberforallthecases.

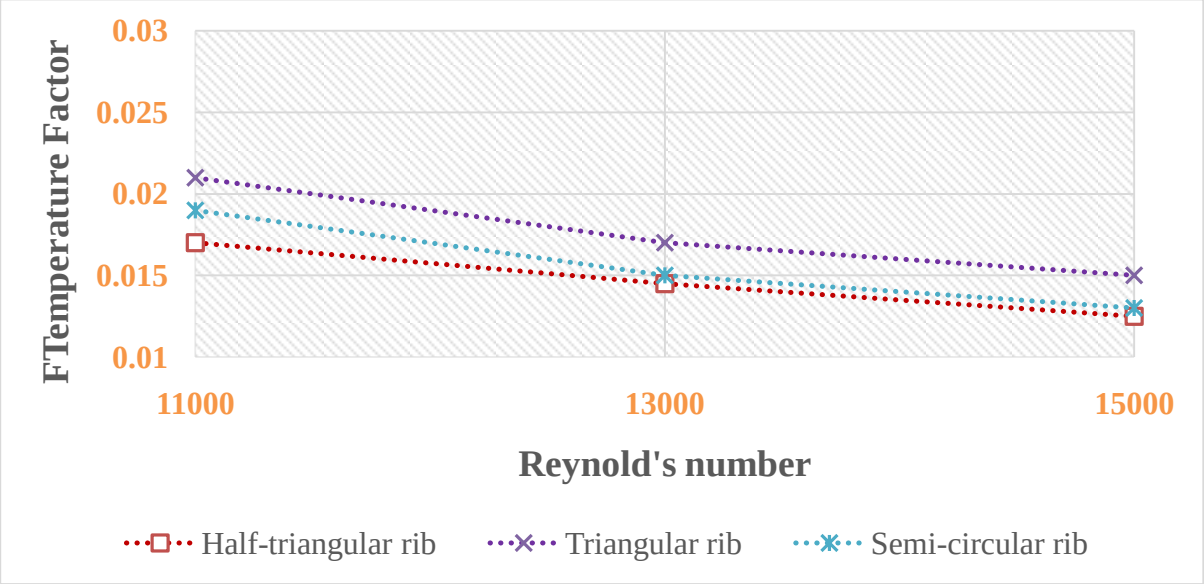

Figure 10. Comparison of the Temperature factor values with half-triangular, triangular, and semi-circular rib on the absorber plate

6. CONCLUSIONS

By studying a 3D curved solar air heater with half-triangular, triangular, and semi-circular rib on the absorber plate rib with the heat transfer and flow friction, the following associated findings may be achieved based on the CFD provision now in operation:

- Triangular-shaped ribs are shown to have the greatest increase in Nusselt number, which is 1.112 times that of half-triangular and corresponds to a Reynolds number of 15,000 for the tested range of parameters.
- For the analysed range of parameters, it is discovered that triangular shaped ribs have the lowest friction factor, which is 0.89 times more than half-triangular ribs.
- For the analysed range of parameters, it is discovered that triangular shaped ribs exhibit the greatest temperature factor augmentation, which is 1.28 times more than that of half-triangular ribs.
- In comparison to half-triangular and semi-circular ribs, it has been discovered that the curved solar air heater with triangular rib roughness on the absorber plate produces better results and may be utilised to promote heat transmission.

REFERENCES

1) Alam, T., and M. H. Kim. 2017. A critical review on artificial roughness provided in rectangular solar air heater duct. Renewable and Sustainable Energy Reviews 69:387–400. doi:10.1016/j.rser.2016.11.192.
2) Kalogirou, S. A., S. Karellas, K. Braimakis, C. Stanciu, and V. Badescu. 2016. Exergy analysis of solar thermal collectors and processes. Progress in Energy and Combustion Science 56:106–37. doi:10.1016/j.pecs.2016.05.002.
3) Sharma, S. K., and V. R. Kalamkar. 2015. Thermo-hydraulic performance analysis of solar air heaters having artificial roughness-A review. Renewable and Sustainable Energy Reviews 41:413–35. doi:10.1016/j.rser.2014.08.051.
4) Arunkumar, H. S., K. V. Karanth, and S. Kumar. 2020. Review on the design modifications of a solar air heater for improvement in the thermal performance. Sustainable Energy Technologies and Assessments 39:100685. doi:10.1016/j. seta.2020.100685.
5) Gabhane, M. G., and A. B. Kanase-Patil. 2017. Experimental analysis of double flow solar air heater with multiple C shape roughness,". Solar Energy 155:1411–16. doi:10.1016/j.solener.2017.07.038.
6) Anil Singh Yadav & J.L. Bhagoria (2017) Numerical investigation of flow through an artificially roughened solar air heater, International Journal of Ambient Energy, 36:2, 87-100, DOI: 10.1080/01430750.2013.823107

7) Alam, T., R. P. Saini, and J. S. Saini. 2014. Effect of circularity of perforation holes in V-shaped blockages on heat transfer and friction characteristics of rectangular solar air heater duct. Energy Conversion and Management 86:952–63. doi:10.1016/j.enconman.2014.06.050.
8) Al-Dabaggah, M., Z. A. H. Obaid, M. Al Qubeissic, D. Dixon-Hardyd, J. Cottome, and P. J. Heggsd. 2015. CFD modeling and performance evaluation of multipass solar air heaters. Numerical Heat Transfer, Part A: Applications 76 (6):438–64. doi:10.1080/10407782.2019.1637228.
9) Poongavanam, G. K., K. Panchabikesan, A. J. D. Leo, and V. Ramalingam. 2018. Experimental investigation on heat transfer augmentation of solar air heater using shot blasted V-corrugated absorber plate. Renewable Energy 127:213–29. doi:10.1016/j.renene.2018.04.056.
10) Yang, Y., and P. Chen. 2014. Numerical study of a solar collector with partitions. Numerical Heat Transfer, Part A: Applications 66 (7):37–41. doi:10.1080/10407782.2014.892330.
11) Gilani, S. E., H. H. Al-Kayiem, D. E. Woldemicheal, and S. I. Gilani. 2017. Performance enhancement of free convective solar air heater by pin protrusions on the absorber. Solar Energy 151:173–85. doi:10.1016/j.solener.2017.05.038.
12) Priyam, A. 2017. Heat transfer and pressure drop characteristics of wavy fin solar air heater. International Journal of Heat and Technology 35 (4):1015–22. doi:10.18280/ijht.350438.
13) Yadav, K. D., and R. K. Prasad. 2020. Performance analysis of parallel flow flat plate solar air heater having arc shaped wire roughened absorber plate. Reinforced Plastics 32:23–44. doi:10.1016/j.ref.2019.10.002.
14) Ajeet PratapSingh ,Akshayveer, Amit Kumar, O.P. Singh. 2020. Efficient design of curved solar air heater integrated with semi-down turbulators. International Journal of Thermal Sciences 152 (2020) 106304.
15) Thakur, S., and N. S. Thakur. 2020. Impact of multi-staggered rib parameters of the 'W' shaped roughness on the performance of a solar air heater channel. Energy Sources, Part A: Recovery, Utilization, and Environmental Effects 1–20. doi:10.1080/15567036.2020.1764672.
16) Wang, L., and B. Sunden. 2007. Experimental investigation of local heat transfer in a square duct with various-shaped ribs. Heat and Mass Transfer 43 (8):759–66. doi:10.1007/s00231-006-0190-y.
17) Webb, R. L., and E. R. Eckert. 1972. Application of rough surfaces to heat exchanger design. International Journal of Heat and Mass Transfer 15 (9):1647–58. doi:10.1016/0017-9310(72)90095-6.
18) Yadav, A. S., and J. L. Bhagoria. 2013a. A CFD (computational fluid dynamics) based heat transfer and fluid flow analysis of a solar air heater provided with circular transverse wire rib roughness on the absorber plate. Energy 55:1127–42. doi:10.1016/j.energy.2013.03.066.
19) Yadav, A. S., and J. L. Bhagoria. 2013b. Heat transfer and fluid flow analysis of solar air heater: A review of CFD approach. Renewable and Sustainable Energy Reviews 23:60–79. doi:10.1016/j.rser.2013.02.035.
20) Yadav, A. S., and J. L. Bhagoria. 2014a. A numerical investigation of square sectioned transverse rib roughened solar air heater. International Journal of Thermal Sciences 79:111–31. doi:10.1016/j.ijthermalsci.2014.01.008.
21) Yadav, A. S., and J. L. Bhagoria. 2014b. A numerical investigation of turbulent flows through an artificially roughened solar air heater. Numerical Heat Transfer, Part A: Applications 65 (7):679–98. doi:10.1080/10407782.2013.846187.
22) Yadav, A. S., and J. L. Bhagoria. 2014c. A CFD based thermo-hydraulic performance analysis of an artificially roughened solar air heater having equilateral triangular sectioned rib roughness on the absorber plate. International Journal of Heat and Mass Transfer 70:1016–39. doi:10.1016/j.ijheatmasstransfer.2013.11.074.